Acta Oceanol. Sin., 2021, Vol. 40, No. 4, P. 136–142
https://doi.org/10.1007/s13131-021-1844-9
http://www.hyxb.org.cn
E-mail: ocean2@hyxb.org.cn

Comparisons of OCO-2 satellite derived XCO_2 with *in situ* and modeled data over global ocean

Siqi Zhang[1, 2, 3], Yan Bai[2, 4], Xianqiang He[2, 4], Haiqing Huang[2], Qiangkun Zhu[2*], Fang Gong[2]

[1] State Key Laboratory of Tropical Oceanography, South China Sea Institute of Oceanology, Chinese Academy of Sciences, Guangzhou 510301, China

[2] State Key Laboratory of Satellite Ocean Environment Dynamics, Second Institute of Oceanography, Ministry of Natural Resources, Hangzhou 310012, China

[3] University of Chinese Academy of Sciences, Beijing 100049, China

[4] Southern Marine Science and Engineering Guangdong Laboratory (Zhanjiang), Zhanjiang 524006, China

Received 7 September 2020; accepted 29 December 2020

Abstract

Atmospheric CO_2 is one of key parameters to estimate air-sea CO_2 flux. The Orbiting Carbon Observatory-2 (OCO-2) satellite has observed the column-averaged dry-air mole fractions of global atmospheric carbon dioxide (XCO_2) since 2014. In this study, the OCO-2 XCO_2 products were compared between *in-situ* data from the Total Carbon Column Network (TCCON) and Global Monitoring Division (GMD), and modeling data from CarbonTracker2019 over global ocean and land. Results showed that the OCO-2 XCO_2 data are consistent with the TCCON and GMD *in situ* XCO_2 data, with mean absolute biases of 0.25×10^{-6} and 0.67×10^{-6}, respectively. Moreover, the OCO-2 XCO_2 data are also consistent with the CarbonTracker2019 modeling XCO_2 data, with mean absolute biases of 0.78×10^{-6} over ocean and 1.02×10^{-6} over land. The results indicated the high accuracy of the OCO-2 XCO_2 product over global ocean which could be applied to estimate the air-sea CO_2 flux.

Key words: XCO_2, OCO-2, comparison, *in situ*, modeling data

Citation: Zhang Siqi, Bai Yan, He Xianqiang, Huang Haiqing, Zhu Qiangkun, Gong Fang. 2021. Comparisons of OCO-2 satellite derived XCO_2 with *in situ* and modeled data over global ocean. Acta Oceanologica Sinica, 40(4): 136–142, doi: 10.1007/s13131-021-1844-9

1 Introduction

Due to the utilization of fossil fuels and changes in land use, atmospheric CO_2 has continued to increase since the industrial revolution, which has profound impact on earth carbon cycle and global warming (IPCC, 2013). Accurate observations of atmospheric CO_2 with high spatiotemporal resolution are the basis for estimating air-sea CO_2 flux (Bai et al., 2015; Song et al., 2016), understanding long-term changes and improving our ability to predict and mitigate climate change (Intergovernmental Panel on Climate Change, 2007; Jenkinson et al., 1991). Understanding the global atmospheric carbon dioxide concentration, especially the atmospheric carbon dioxide change over the ocean, is an important reference for many global climate changes above. Currently, there are several ways to obtain dry-air mole fractions of atmospheric CO_2 (XCO_2), including *in situ* measurements, remote sensing and modeling simulation. *In situ* measurements generally provide the best quality CO_2 concentrations, but the number of ground-based sites is limited, resulting in the absence of data in many global areas, especially in oceanic regions (Bousquet et al., 2006; Eldering et al., 2017). In contrast, spaceborne detection is the most effective technical method to observe atmospheric XCO_2 with long time series and global coverage. For example, the Scanning Imaging Absorption Spectrometer for Atmospheric Chartography launched in 2002 was the first space-based instrument to retrieve atmospheric XCO_2 (Bovensmann et al., 1999; Buchwitz et al., 2007). Launched in April 2009, the Greenhouse Gases Observing Satellite (GOSAT) provides a more accurate atmospheric XCO_2 product, at a precision of around 0.6% (Cogan et al., 2012; Joiner et al., 2011; Yokota et al., 2009), as does GOSAT-2, which was launched in October 2018. Especially, NASA launched the Orbiting Carbon Observatory-2 (OCO-2) on 2 July 2014 to provide an atmospheric XCO_2 product with higher accuracy (Crisp, 2015). In addition, China launched TANSAT satellite in December 2016 to measure atmospheric XCO_2.

Satellite remote sensing of atmospheric XCO_2 is still in the developing stage, especially in regard to validation of satellite-derived XCO_2 products on a global scale. The principal challenge is the need for unprecedented levels of precision and accuracy to resolve long-term changes and quantify CO_2 flux; however, as an indirect observation, the accuracy of satellite detection is limited by inversion algorithms. Moreover, the validation of XCO_2 products often relies on limited *in situ* measurements. Based on prospective application in three sites, Connor et al. (2008) found

Foundation item: The National Key Research and Development Programme of China under contract No. 2017YFA0603004; the Fund of Southern Marine Science and Engineering Guangdong Laboratory (Zhanjiang) (Zhanjiang Bay Laboratory) under contract No. ZJW-2019-08; the National Natural Science Foundation of China under contract Nos 41825014, 41676172 and 41676170; the Global Change and Air-Sea Interaction Project of China under contract Nos GASI-02-SCS-YGST2-01, GASI-02-PACYGST2-01 and GASI-02-IND-YGST2-01.

*Corresponding author, E-mail: zhuqiankun@sio.org.cn

expected errors in the OCO inverse method of less than 1×10^{-6} for all conditions. Boesch et al. (2011) found that satellite-retrieved XCO_2 is sensitive to solar zenith angle, with errors typically less than 1×10^{-6} for nadir or glint mode, but which increase to around 3×10^{-6} for the large solar zenith angles. Research has also shown that the *in situ* XCO_2 values obtained from the Total Carbon Column Observing Network (TCCON) agree well with those obtained from OCO-2, with absolute median difference of less than 0.5×10^{-6} and root mean square error (RMSE) of less than 1.5×10^{-6} (Wunch et al., 2017).

In this study, the OCO-2 XCO_2 products were comprehensively compared between *in situ* data from TCCON and Global Monitoring Division (GMD) and modeling data from CarbonTracker2019 (Dlugokencky et al., 2019; Jacobson et al., 2020). Section 2 presents the data preparation and matchup methods. Section 3 provides the comparison results and analyzes of difference among diverse data sets over the global area. Finally, the summary and conclusions are given in Section 4.

2 Data and methods

2.1 *OCO-2 XCO_2 product*

The OCO-2-retrieved Level-2 XCO_2 product with reprocessing version 9 from the GES-DISC platform (http://disc.sci.gsfc.nasa.gov) was obtained. The level-2 product provides relatively stable spatial coverage and efficient data (Liang et al., 2017). The column-averaged CO_2 dry air mole fraction XCO_2 was retrieved from the hyper-spectral radiance measured by the OCO-2. It was found that the effect of the water vapor absorption on the OCO-2 measured radiance spectra is indeed weak (Boesch et al., 2015). In addition, for the parameters relative to humidity in the XCO_2 retrieval algorithm, both the wet and dry contributions were concerned, such as the Rayleigh optical depth. This product has a spatial resolution of 2.25 km×1.29 km with bias correction. Quality flags are included in the product, which can assist the user in selecting high-quality data. In this study, OCO-2 XCO_2 data from January 2015 to December 2018 with a quality flag value of zero were used, corresponding to the highest quality data.

2.2 *CarbonTracker modeling XCO_2 data*

CarbonTracker provides four-dimensional (4-D) (i.e., time and three dimensional space) XCO_2 data. The CarbonTracker modeling data are based on global *in situ* observations of atmospheric XCO_2 and TM5 model simulation of CO_2 transportation on the earth's surface (Peters et al., 2007). It estimates exchanges between the various carbon reservoirs, i.e., land biosphere, ocean, atmosphere, and fossil fuels. The latest CarbonTracker modeling XCO_2 data (i.e., CarbonTracker2019) were obtained from the GMD platform (https://esrl.noaa.gov/gmd/ccgg/carbontracker). CarbonTracker2019 provides daily global XCO_2 data and CO_2 mole fractions at 25 vertical layers with a spatial resolution of 2° (latitude) × 3° (longitude). CarbonTracker2019 data from January 2015 to December 2018 were used (corresponding to the end date of CarbonTracker2019 at the current stage).

In terms of matchup between OCO-2 XCO_2 and CarbonTracker modeling data, the modeling data were resampled to a spatial resolution of 0.5° based on cubic spline interpolation. And then, this study matched the OCO-2 XCO_2 with the resampled modeling data based on same day and location.

2.3 *TCCON in situ XCO_2 data*

The TCCON is a global network of ground-based Fourier-transformed spectrometers that record near-infrared solar absorption spectra (Wunch et al., 2011). From these spectra, accurate and precise column-averaged abundances of CO_2 can be retrieved. The newest version of TCCON XCO_2 data were obtained from the platform (https://tccondata.org). TCCON provides ground-based column-averaged XCO_2 data. In this study, the column-averaged XCO_2 from 34 global TCCON sites from 2015 to 2018 were used, corresponding to the period of obtained OCO-2 XCO_2 product (Blumenstock et al., 2014; De Mazière et al., 2017; Griffith et al., 2014a, b; Hase et al., 2017; Iraci et al., 2016a, b; Kawakami et al., 2014; Kivi et al., 2014; Notholt et al., 2014, 2017; Sherlock et al., 2014a, b; Strong et al., 2017). This study used a ±0.2 h temporal window and 110 km spatial window to match the OCO-2-derived XCO_2 and TCCON-measured XCO_2. Overall, total 2 473 matchups over global ocean and land were obtained, and Fig. 1 shows the distribution of TCCON sites with matchups to OCO-2-retrieved XCO_2.

2.4 *GMD in situ data*

The GMD *in situ* CO_2 data were obtained from the NOAA-GMD platform (https://www.esrl.noaa.gov/gmd). The *in situ* measurement uses automated portable sampler to collect air samples. Air samples are collected approximately weekly from a globally distributed network of stations. A condenser has been added to remove a significant amount of water vapor from the sample by cooling the air stream. This change will improve the CO_2 measurements from samples collected at humid tropical loc-

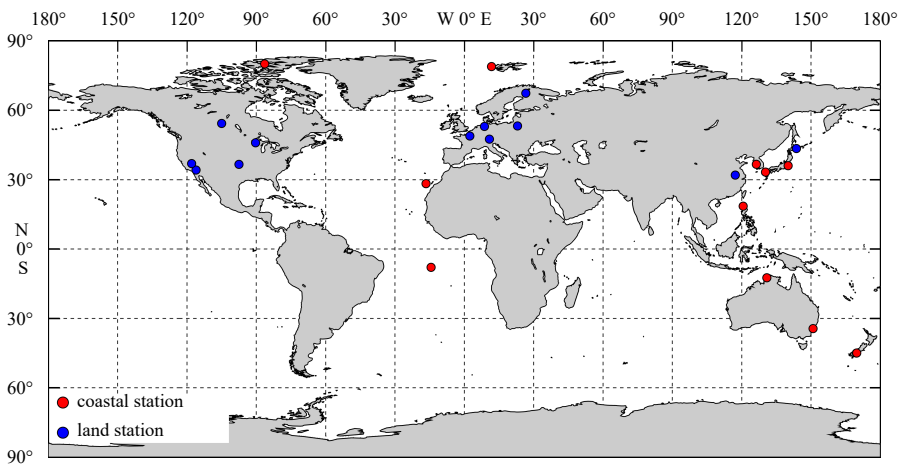

Fig. 1. Locations of the Total Carbon Column Observing Network stations with matchups to OCO-2 XCO_2 products.

ations. The *in situ* data were from 143 stations and included geographic, time, measurement details and other auxiliary information. GMD data from January 2015 to December 2018 were obtained, corresponding to the period of the obtained OCO-2 XCO_2 product. Quality control was applied in the GMD CO_2 data, and only "pass" records with rejection, selection, and information flags were used for further comparison.

It should be noted that GMD CO_2 was measured at the bottom layer of the atmosphere. To compare the OCO-2-retrieved XCO_2 column values, the GMD CO_2 data were converted to column XCO_2. The averaging kernel method was used to convert GMD measured CO_2 (XCO_{2_GMD}) to column XCO_2 (Connor et al., 2008) as:

$$XCO_{2\_gmd} = XCO_{2\_prior} + \sum_{i}^{n} h_i a_i (H(x) - X_a)_i,$$

where XCO_{2_prior}, a_i, and X_a represent priori, column averaging kernel, and profile values, respectively, which can all be obtained from the satellite product; h is the pressure weighting function; and i is the height level. The profile of the CO_2 mole fractions (25 levels) from the CarbonTracker modeling and GMD CO_2 data was used to obtain the key parameter $H(x)$, which maps the 26 levels of CO_2 mole fractions. By combining the bottom CO_2 from GMD and vertical profile of CO_2 (25 layers) from CarbonTracker to form a 26 layer CO_2 profile, the GMD CO_2 was thus converted into column XCO_2 as measured by OCO-2.

This study used ±5 h temporal windows to match OCO-2 and GMD XCO_2, resulting in a time difference between OCO-2 observation and GMD measurement of less than 5 h. The distance of the matchup should also be less than 100 km. It should be noted that for cases of multiple OCO-2 XCO_2 pixels matching one *in situ* sample, the average XCO_2 value for all matchup pixels was used for further comparison. Figure 2 shows the distributions of GMD stations with matchups to OCO-2 XCO_2 data. Overall, the matchup stations cover different regions of both global land and ocean, except the Antarctic.

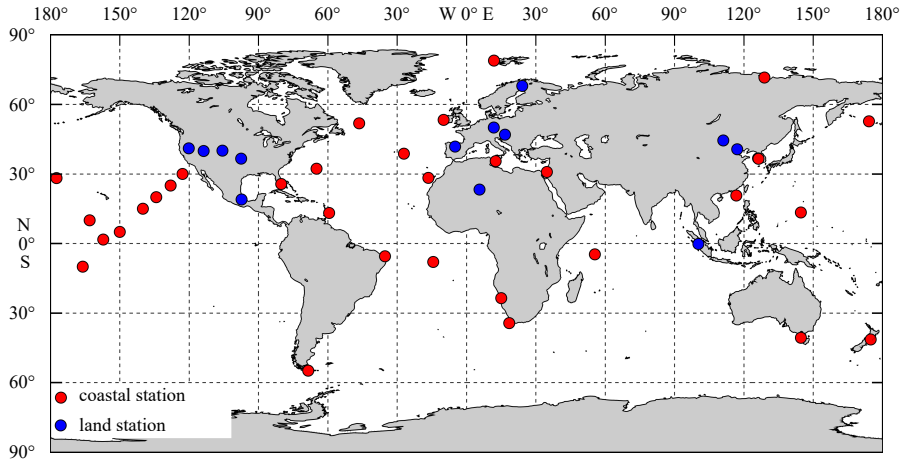

Fig. 2. Locations of the Global Monitoring Division stations with matchups to OCO-2 XCO_2 products.

3 Results and discussion

3.1 *Comparisons between OCO-2 and TCCON XCO_2*

Compared to the TCCON-measured XCO_2, the OCO-2 retrieved XCO_2 showed a mean absolute difference of 0.247×10^{-6}, RMSE of 1.141×10^{-6}, and correlation coefficient (R) of 0.958 for all matchups in global ocean and land, indicating good performance of the OCO-2-retrieved XCO_2 product (Fig. 3). Moreover, the OCO-2 retrieved XCO_2 showed better performance in the ocean (compared with TCCON coastal sites) than it in the land (compared with TCCON terrestrial sites), as shown in Fig. 4. Specifically, for the coastal sites, the mean absolute difference is 0.121×10^{-6} with RMSE of 1.035×10^{-6} and R of 0.965, while it is 0.412×10^{-6} with RMSE of 1.244×10^{-6} and R of 0.953 for land sites. Therefore, it is obvious that OCO-2 XCO_2 product has better consistency between satellite retrieval and *in situ* data in the oceanic region, which is expected to be related to the different retrieval algorithm and complexity of underlying surface.

Based on TCCON-measured data from 2014 to 2016, Wunch et al. (2017) found OCO-2 XCO_2 was consistent with global TCCON XCO_2 from September 2014 to April 2016, with a median difference of less than 0.5×10^{-6}, RMSE typically below 1.5×10^{-6}, and R of 0.911. Liang et al. (2017) also reported an overall bias between OCO-2 and TCCON XCO_2 of $(0.267\ 1\pm1.56)\times10^{-6}$ from September 2014 to December 2016, with R of 0.879. Overall, our

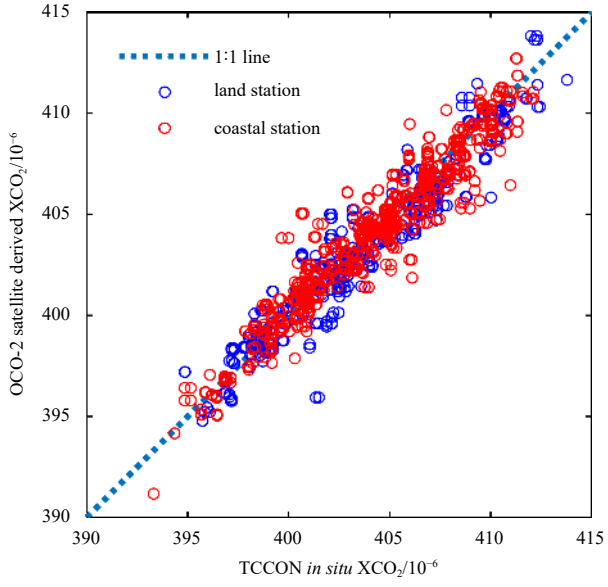

Fig. 3. Comparison between OCO-2-retrieved XCO_2 and the Total Carbon Column Observing Network (TCCON) *in situ* measurements. Red and blue points are the matchups for the oceanic and land stations, respectively. Blue dashed line represents the 1:1 line.

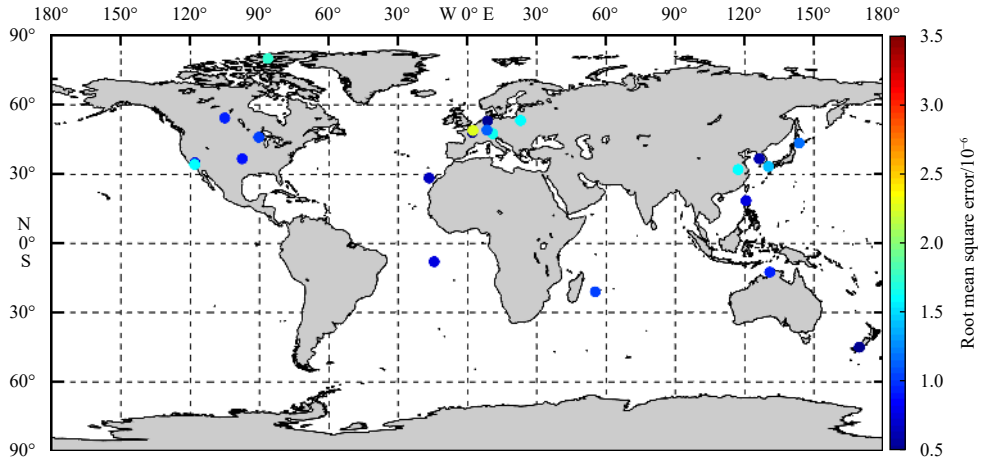

Fig. 4. The global distribution of root mean square error between OCO-2 and TCCON XCO_2 at each station.

validation results are consistent with those of previous studies, and the slight differences are likely caused by the extended period of TCCON XCO_2 from 2015 to 2018 in this study.

3.2 *Comparisons between OCO-2 XCO_2 and GMD data*

Figure 5 presents the comparisons between the OCO-2 and GMD XCO_2 values. Clearly, OCO-2 XCO_2 demonstrated good performance compared with GMD XCO_2, with a mean absolute difference of 0.672×10^{-6}, RMSE of 1.684×10^{-6}, and R of 0.865. This accuracy is comparable to the validation results between the Greenhouse Gases Observing Satellite (GOSAT) and TCCON-measured XCO_2, with a mean absolute difference of less than 0.4×10^{-6} (Maki et al., 2010) when considering the discrepancy between mean and mean absolute differences.

Similar to the comparison result with the TCCON XCO_2, OCO-2 XCO_2 product showed better performance over ocean (mean absolute difference of 0.441×10^{-6}, RMSE of 1.306×10^{-6}, and

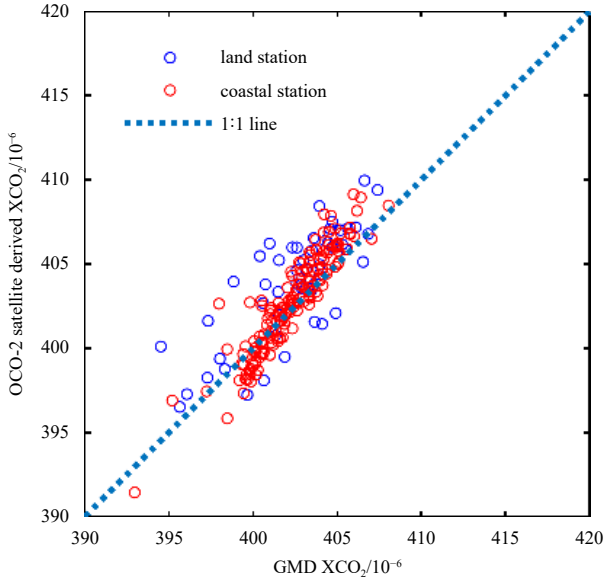

Fig. 5. The blue plots show the comparison between OCO-2-retrieved XCO_2 and the Global Monitoring Division (GMD) XCO_2 at different GMD terrestrial stations; red one for comparison between OCO-2-retrieved and GMD XCO_2 over coastal station; dashed blue line represents 1:1 line.

R of 0.924) than over land (mean absolute difference of 1.372×10^{-6}, RMSE of 2.474×10^{-6}, and R of 0.776) as comparing with the GMD data (Fig. 6). The discrepancy between OCO-2 and GMD XCO_2 values reached 5×10^{-6} at some GMD stations on the land. This large discrepancy was likely due to the following reasons. First, there are several GMD stations located in complex terrains with significant spatial variability in topography or ground cover. Therefore, the low spatial resolution of the OCO-2 XCO_2 product and the matchup windows with100 km for space and ±5 h for time may not be suitable for these stations. Although using stricter matchup windows could result in better performance, the number of effective matchups would also be reduced, making it difficult to achieve a representative assessment. Second, the modeling profiles and *in-situ* data to the OCO-2 XCO_2 observation space were mapped to estimate GMD XCO_2, which may contain some uncertainty.

It should be noted that OCO-2-retrieved XCO_2 exhibited slight overestimation at low XCO_2 and underestimation at high XCO_2 compared to the GMD XCO_2. This effect is likely caused by the different spatial resolutions between OCO-2 and GMD measurements, since OCO-2 XCO_2 is the averaged value of 2.25 km× 1.29 km, while GMD XCO_2 is obtained at a specific site.

Although the matchup stations might be not large enough for the global distribution which comes from two reasons. The one is limited of XCO_2 ground-based sites, and they are mainly distributed in developed regions (usually densely populated areas). The other reason is that the satellite is along-track observation causing the low spatial resolution of the XCO_2 products.

3.3 *Comparisons between OCO-2 and CarbonTracker XCO_2*

Figures 7a and b show comparisons between OCO-2-retrieved and CarbonTracker-modeled XCO_2 values over land and ocean, respectively. In general, the CarbonTracker modeling results were consistent with the OCO-2-retrieved XCO_2, with R of 0.897 for land and 0.945 for ocean. Thus, the CarbonTracker XCO_2 product showed better performance over the ocean (mean absolute difference of 0.779×10^{-6}, RMSE of 0.990×10^{-6}) than over land (mean absolute difference of 1.023×10^{-6}, RMSE of 1.399×10^{-6}). The relatively larger discrepancy between CarbonTracker modeling and OCO-2 XCO_2 over land was expected to be caused by higher inhomogeneity of XCO_2 over land than over ocean. The spatial resolution of the CarbonTracker-modeled XCO_2 is rather coarse (3° in longitude and 2° in latitude). In oceanic regions, XCO_2 is relatively spatially uniform, and the effect of coarse resolution on the matchup between CarbonTracker-modeled and OCO-2-obtained XCO_2 is therefore limited. However, over land

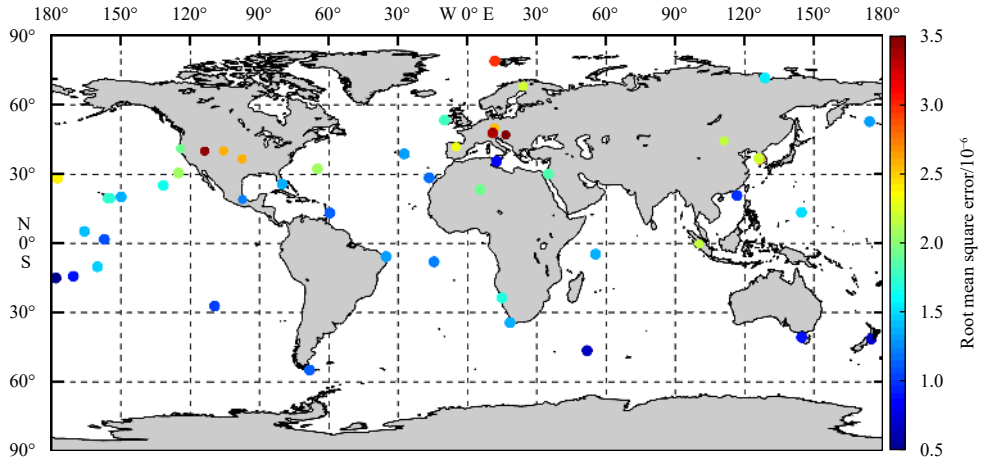

Fig. 6. The global distribution of root mean square error between GMD and OCO-2 XCO2 at each station.

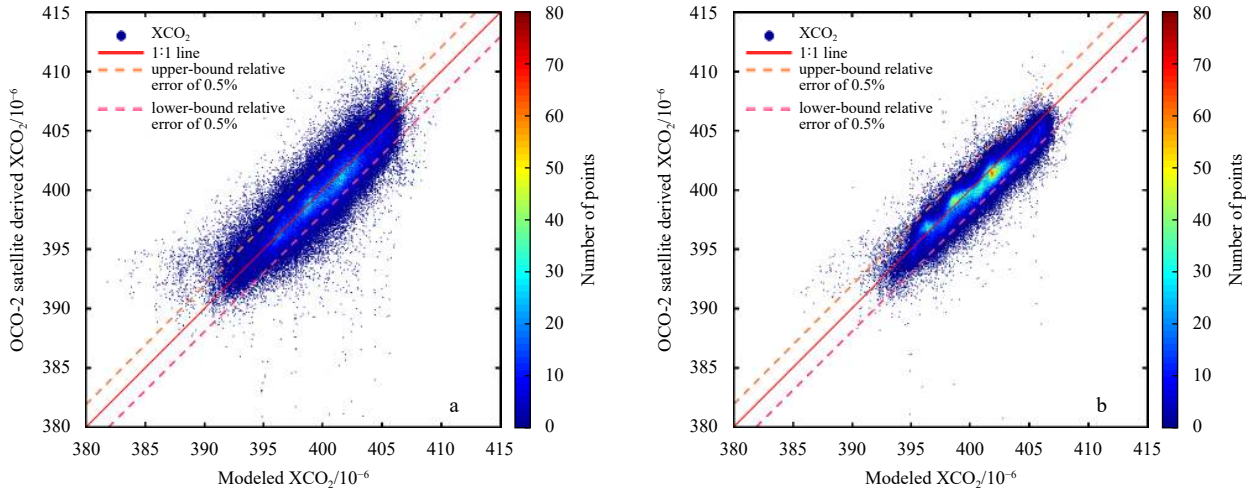

Fig. 7. Comparison between OCO-2-retrieved and CarbonTracker-modeled XCO_2. a. Comparison over land; b. comparison over ocean. Solid red line represents 1:1 line and dashed red line represents relative error of 0.5%. Color bar shows number of points.

regions, especially with high spatial inhomogeneity, the effect of coarse resolution could be significant, which might result in relatively low agreement between CarbonTracker and OCO-2 XCO_2. To quantitatively analyze the differences between OCO-2 and CarbonTracker XCO_2, their differences, i.e., d-XCO_2 (d-XCO_2= $XCO_{2(CarbonTracker)}$–$XCO_{2(OCO-2)}$), were determined from 2015 to 2018. Overall, d-XCO_2 demonstrated near Gaussian distribution, with a mean value of -0.37×10^{-6} and standard deviation of 1.04×10^{-6}. If the matchups between two datasets were divided into two groups according to the underlying surface type (land or ocean), the mean d-XCO_2 for ocean was -0.17×10^{-6} (standard deviation of 0.93×10^{-6}) and for land was -0.47×10^{-6} (standard deviation of 1.18×10^{-6}).

Figure 8 showed the spatial distribution of d-XCO_2 at the global scale. Clearly, d-XCO_2 over ocean regions demonstrated obviously discrepancies between the Northern Hemisphere (NH) and Southern Hemisphere (SH). Overall, oceanic d-XCO_2 was higher in the NH than in the SH. When taking OCO-2 XCO_2 as a reference, the CarbonTracker-modeled XCO_2 in the NH exhibited slight underestimation over ocean regions and slight overestimation over land regions, especially in central Asia and equatorial areas. However, in the SH, the CarbonTracker XCO_2 demonstrated slight overestimation over ocean regions, except at high latitudes. If 0.3% of all points, which have the largest absolute value of d-XCO_2, were extract, the underestimation of XCO_2 by CarbonTracker occurred more frequently in the mid- and low-latitude areas in the NH, especially oceanic regions, whereas the overestimation of XCO_2 by CarbonTracker occurred more often over land regions. Northcott et al. (2019) also found greatly enhanced atmospheric CO_2 levels relative to well-mixed marine atmosphere were observed during periods of offshore winds at coastal sensor platforms, which could not be exhibited by CarbonTracker.

Interestingly, there is a clear boundary for the d-XCO_2 in the ocean and the land. CarbonTracker uses an offline atmospheric transport model and four surface flux modules representing four crucial CO_2 transmissions. The 4-D results are interpolated for the times and locations where atmospheric observations exist, and initial net surface fluxes are adjusted using a set of weekly and regional flux scaling factors to minimize differences between the forecasted and observed CO_2 mole fractions using an ensemble Kalman filter optimization scheme with a five week lag (Williams et al., 2014). This model has certain deviations in the simulation of different underlying surfaces, and the significant gap between land and ocean does not appear to be due to a faulty gas transport model and coarse spatial resolution. These deviations are more likely from incorrect estimation of input parameters (like net ecosystem exchange) to the four surface flux

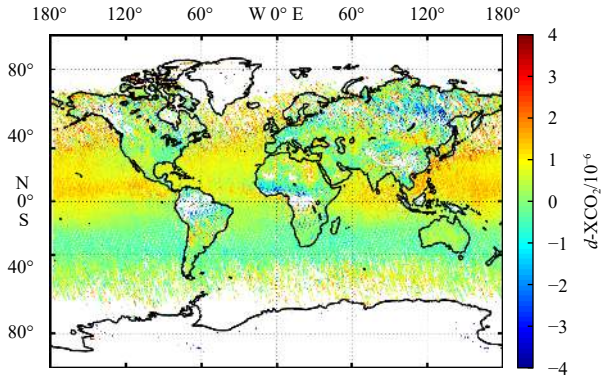

Fig. 8. Global distribution of mean differences between OCO-2 XCO_2 and CarbonTracker XCO_2 (d-XCO_2=$XCO_{2(CarbonTracker)}$−$XCO_{2(OCO-2)}$).

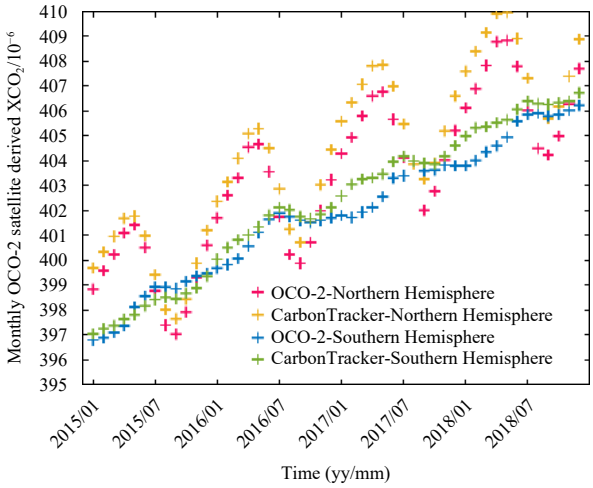

Fig. 9. Temporal variations of the monthly XCO_2 of OCO-2-derived and CarbonTracker in low-moderate latitude areas (less than 45°) in Southern Hemisphere and Northern Hemisphere from January 2015 to December 2018.

modules, especially a priori net ocean surface fluxes. Although large oceanic fluxes are observed in tropical and extra-tropical oceanic regions, these values are one order of magnitude smaller than that of bio-flux emissions (Maki et al., 2010). Of course, the coarse spatial resolution of CarbonTracker may also be a possible reason why the model was unsatisfactory in simulating extreme values. In addition, the differences in the representative heights of the satellite-measured and modeled XCO_2 could induce variance between them. This effect could partly explain the underestimation and overestimation of the modeled XCO_2 over the ocean and land areas of the NH, respectively. In the ocean regions, the glint model adopted by the satellite measurement will enhance the weight of low atmosphere layers with high CO_2, which could result in higher XCO_2 by satellite measurement. In contrast, the nadir model by satellite measurement over land will enhance the weight of upper atmosphere layers with low CO_2, resulting in lower XCO_2 by satellite measurement.

To determine the differences in temporal variations between OCO-2 and CarbonTracker XCO_2, the monthly average values were calculated over 2015–2018 in low-moderate latitude areas (0°–45°) in the SH and NH, respectively (Fig. 9). Overall, the CarbonTracker-modeled XCO_2 exhibited systematically higher values than the OCO-2-derived XCO_2 in the NH, and the differences increased from 0.61×10^{-6} in 2015 to 1.28×10^{-6} in 2018, and an increase in the amplitude of seasonal XCO_2 change could be found in the high latitude areas of the NH. Some of the previously studies pointed out that these trend are primarily driven by forest expansion and increased natural vegetation growth (Forkel et al., 2016; Graven et al., 2013), while others suggested that agricultural expansion and intensification result in increased productivity and thus enhance the seasonal variations in cultivated areas at mid-latitude regions (Gray et al., 2014; Zeng et al., 2014). In the SH, the modeled data showed smaller seasonal fluctuations than the OCO-2 XCO_2 data. The SH is not considered as the main emission area of CO_2, so it is also significance to consider the impact of different seasonal atmospheric circulation on the XCO_2 variation (Grise and Polvani, 2017). In particular, the overestimation of the modeled data showed remarkably increase from the middle of 2016 in the SH, especially in February (0.34×10^{-6} in February 2015, 0.69×10^{-6} in February 2016, 1.34×10^{-6} in February 2017, 1.32×10^{-6} in February 2018). By analyzing the February data in 2017–2018, the largest discrepancy between the modeled and OCO-2-derived XCO_2 mainly occurred in the Sahara Desert, which might be induced by uncertainty in biological flux (Williams et al., 2014).

4 Conclusions

This study compared the OCO-2 XCO_2 product with *in situ* data from TCCON and GMD measurements and with CarbonTracker modeling. OCO-2 XCO_2 was consistent with TCCON-measured XCO_2, with a mean absolute difference of 0.247×10^{-6} and RMSE of 1.141×10^{-6}. Compared with the GMD-derived XCO_2, the OCO-2-retrieved XCO_2 had a mean absolute difference of 0.672×10^{-6} and RMSE of 1.684×10^{-6}. These high agreements showed that the OCO-2 could provide high quality XCO_2 data over the low-moderate latitude regions. Moreover, the comparison between satellite and moldering product showed that they were relatively consistent with each other, with a mean absolute difference of 1.02×10^{-6} over land and 0.78×10^{-6} over ocean. In addition, the comparison results showed that the agreement among three different types dataset of XCO_2 was higher in the oceanic area than it in the terrestrial area, indicating the high applicable of the OCO-2-retrieved XCO_2 product to estimate the air-sea CO_2 flux over ocean. Our results also evidenced the reliable of the CarbonTracker modeling XCO_2 data, and with the advantage of the global coverage, this modeling data can also be used to estimate the air-sea CO_2 flux over ocean when satellite product is unavailable.

Acknowledgements

We thank NASA for providing the OCO-2 XCO_2 product, Caltech Library Research Data Repository for providing TCCON XCO_2 data, and NOAA ESRL, Boulder, Colorado, USA for providing the GMD *in situ* data and CarbonTracker modeling data. We thank the satellite ground station, satellite data processing and sharing center, and marine satellite data online analysis platform (SatCO2) of SOED/SIO/MNR for help with data collection and processing.

References

Bai Yan, Cai Weijun, He Xianqiang, et al. 2015. A mechanistic semi-analytical method for remotely sensing sea surface pCO_2 in river-dominated coastal oceans: A case study from the East China Sea. Journal of Geophysical Research: Oceans, 120(3): 2331–2349, doi: 10.1002/2014JC010632

Blumenstock T, Hase F, Schneider M, et al. 2014. TCCON data from Izana (ES), Release GGG2014R0. https://data.caltech.edu/records/293 [2017-09-13/2018-04-19]

Boesch H, Baker D, Connor B, et al. 2011. Global characterization of CO_2 column retrievals from shortwave-infrared satellite observations of the Orbiting Carbon Observatory-2 mission. Remote Sensing, 3(2): 270–304, doi: 10.3390/rs3020270

Boesch H, Brown L, Castano R, et al. 2015. Orbiting Carbon Observatory (OCO)-2. https://docserver.gesdisc.eosdis.nasa.gov/public/project/OCO/OCO2_L2_ATBD.V6.pdf [2018-01-21/2018-09-16]

Bousquet P, Ciais P, Miller J, et al. 2006. Contribution of anthropogenic and natural sources to atmospheric methane variability. Nature, 443(7110): 439–443, doi: 10.1038/nature05132

Bovensmann H, Burrows J P, Buchwitz M, et al. 1999. SCIAMACHY: Mission objectives and measurement modes. Journal of the Atmospheric Sciences, 56(2): 127–150, doi: 10.1175/1520-0469(1999)056<0127:SMOAMM>2.0.CO;2

Buchwitz M, Schneising O, Burrows J P, et al. 2007. First direct observation of the atmospheric CO_2 year-to-year increase from space. Atmospheric Chemistry and Physics, 7(16): 4249–4256, doi: 10.5194/acp-7-4249-2007

Cogan A J, Boesch H, Parker R J, et al. 2012. Atmospheric carbon dioxide retrieved from the Greenhouse gases observing satellite (GOSAT): Comparison with ground-based TCCON observations and GEOS-Chem model calculations. Journal of Geophysical Research: Atmospheres, 117(D21): D21301

Connor B J, Boesch H, Toon G, et al. 2008. Orbiting Carbon Observatory: Inverse method and prospective error analysis. Journal of Geophysical Research: Atmospheres, 113(D5): D05305

Crisp D. 2015. Measuring atmospheric carbon dioxide from space with the orbiting carbon observatory-2(OCO-2). In: Proceedings of SPIE 9607, Earth Observing Systems XX. San Diego, United States: SPIE, 960702

De Mazière M, Sha M K, Desmet F, et al. 2017. TCCON data from Réunion Island (RE), Release GGG2014. R1. https://data.caltech.edu/records/293 [2017-09-13/2018-04-19]

Dlugokencky E, Mund J W, Crotwell A M, et al. 2019. Atmospheric Carbon Dioxide Dry Air Mole Fractions from the NOAA ESRL Carbon Cycle Cooperative Global Air Sampling Network, 1968–2018. Boulder, USA: NOAA ESRL Global Monitoring Division

Eldering A, O'Dell C W, Wennberg P O, et al. 2017. The Orbiting Carbon Observatory 2: First 18 months of science data products. Atmospheric Measurement Techniques, 10(2): 549–563, doi: 10.5194/amt-10-549-2017

Forkel M, Carvalhais N, Rödenbeck C, et al. 2016. Enhanced seasonal CO2 exchange caused by amplified plant productivity in northern ecosystems. Science, 351(6274): 696–699, doi: 10.1126/science.aac4971

Graven H D, Keeling R F, Piper S C, et al. 2013. Enhanced seasonal exchange of CO_2 by northern ecosystems since 1960. Science, 341(6150): 1085–1089, doi: 10.1126/science.1239207

Gray J M, Frolking S, Kort E A, et al. 2014. Direct human influence on atmospheric CO_2 seasonality from increased cropland productivity. Nature, 515(7527): 398–401, doi: 10.1038/nature13957

Griffith D W T, Deutscher N M, Velazco V A, et al. 2014a. TCCON data from Darwin (AU), Release GGG2014R0. https://data.caltech.edu/records/293 [2017-09-13/2018-04-19]

Griffith D W T, Velazco V A, Deutscher N M, et al. 2014b. TCCON data from Wollongong (AU), Release GGG2014R0. https://data.caltech.edu/records/293 [2017-09-13/2018-04-19]

Grise K M, Polvani L M. 2017. Understanding the time scales of the tropospheric circulation response to abrupt CO_2 forcing in the Southern Hemisphere: seasonality and the role of the stratosphere. Journal of Climate, 30(21): 8497–8515, doi: 10.1175/JCLI-D-16-0849.1

Hase F, Blumenstock T, Dohe S, et al. 2017. TCCON data from Karlsruhe (DE), Release GGG2014R1. https://data.caltech.edu/records/293 [2017-09-13/2018-04-19]

Intergovernmental Panel on Climate Change. 2007. Climate Change 2007: the Physical Science Basis: Working Group I Contribution to the Fourth Assessment Report of the IPCC. Cambridge: Cambridge University Press, 847–940

IPCC. 2013. Climate Change 2013: The Physical Science Basis. Working Group I Contribution to the Fifth Assessment Report of the Intergovernmental Panel on Climate Change. Cambridge: Cambridge University Press

Iraci L T, Podolske J, Hillyard P W, et al. 2016a. TCCON data from Edwards (US), Release GGG2014R1, Pasadena, California. https://data.caltech.edu/records/293 [2017-09-13/2018-04-19]

Iraci L T, Podolske J, Hillyard P W, et al. 2016b. TCCON data from Indianapolis (US), Release GGG2014R1, Pasadena, California. https://data.caltech.edu/records/293 [2017-09-13/2018-04-19]

Jacobson A R, Schuldt K N, Miller J B, et al. 2020. CarbonTracker CT2019. NOAA Earth System Research Laboratory, Global Monitoring Division. https://gml.noaa.gov/ccgg/carbontracker/CT2019/CT2019_doc.php [2018-04-19]

Jenkinson D S, Adams D E, Wild A. 1991. Model estimates of CO_2 emissions from soil in response to global warming. Nature, 351(6324): 304–306, doi: 10.1038/351304a0

Joiner J, Yoshida Y, Vasilkov A, et al. 2011. First observations of global and seasonal terrestrial chlorophyll fluorescence from space. Biogeosciences, 8(3): 637–651, doi: 10.5194/bg-8-637-2011

Kawakami S, Ohyama H, Arai K, et al. 2014. TCCON data from Saga (JP), Release GGG2014R0. https://data.caltech.edu/records/293 [2017-09-13/2018-04-19]

Kivi R, Heikkinen P, Kyr. 2014. TCCON data from Sodankyla (FI), Release GGG2014R0. 637–651. https://data.caltech.edu/records/293 [2017-09-13/2018-04-19]

Liang A L, Gong W, Han G, et al. 2017. Comparison of satellite-observed XCO_2 from GOSAT, OCO-2, and ground-based TCCON. Remote Sensing, 9(10): 1033, doi: 10.3390/rs9101033

Maki T, Ikegami M, Fujita T, et al. 2010. New technique to analyse global distributions of CO_2 concentrations and fluxes from non-processed observational data. Tellus B, 62(5): 797–809, doi: 10.1111/j.1600-0889.2010.00488.x

Northcott D, Sevadjian J, Sancho-Gallegos D A, et al. 2019. Impacts of urban carbon dioxide emissions on sea-air flux and ocean acidification in nearshore waters. PLoS One, 14(3): e0214403, doi: 10.1371/journal.pone.0214403

Notholt J, Petri C, Warneke T, et al. 2014. TCCON data from Bremen (DE), Release GGG2014R0. https://data.caltech.edu/records/293 [2017-09-13/2018-04-19]

Notholt J, Warneke T, Petri C, et al. 2017. TCCON data from Ny Ålesund, Spitsbergen (NO), Release GGG2014. R0. https://data.caltech.edu/records/293 [2017-09-13/2018-04-19]

Peters W, Jacobson A R, Sweeney C, et al. 2007. An atmospheric perspective on North American carbon dioxide exchange: CarbonTracker. Proceedings of the National Academy of Sciences of the United States of America, 104(48): 18925–18930, doi: 10.1073/pnas.0708986104

Sherlock V, Connor B J, Robinson J, et al. 2014a. TCCON data from Lauder (NZ), 120HR, Release GGG2014R0. https://data.caltech.edu/records/293 [2017-09-13/2018-04-19]

Sherlock V, Connor B J, Robinson J, et al. 2014b. TCCON data from Lauder (NZ), 125HR, Release GGG2014R0. https://data.caltech.edu/records/293 [2017-09-13/2018-04-19]

Song Xuelian, Bai Yan, Cai Weijun, et al. 2016. Remote sensing of sea surface pCO_2 in the bering sea in summer based on a Mechanistic Semi-Analytical Algorithm (MeSAA). Remote Sensing, 8(7): 558, doi: 10.3390/rs8070558

Strong K, Mendonca J, Weave D, et al. 2017. TCCON data from Eureka (CA), Release GGG2014R1. https://data.caltech.edu/records/293 [2017-09-13/2018-04-19]

Williams I N, Riley W J, Torn M S, et al. 2014. Biases in regional carbon budgets from covariation of surface fluxes and weather in transport model inversions. Atmospheric Chemistry and Physics, 14(3): 1571–1585, doi: 10.5194/acp-14-1571-2014

Wunch D, Toon G C, Blavier J F L, et al. 2011. The total carbon column observing network. Philosophical Transactions. Series A: Mathematical, Physical, and Engineering Sciences, 369(1943): 2087–2112

Wunch D, Wennberg P O, Osterman G, et al. 2017. Comparisons of the orbiting carbon observatory-2(OCO-2) XCO_2 measurements with TCCON. Atmospheric Measurement Techniques, 10: 2209–2238, doi: 10.5194/amt-10-2209-2017

Yokota T, Yoshida Y, Eguchi N, et al. 2009. Global concentrations of CO_2 and CH_4 retrieved from GOSAT: First preliminary results. Sola, 5: 160–163, doi: 10.2151/sola.2009-041

Zeng Ning, Zhao Fang, Collatz G J, et al. 2014. Agricultural green revolution as a driver of increasing atmospheric CO_2 seasonal amplitude. Nature, 515(7527): 394–397, doi: 10.1038/nature13893